Deprotonation Mechanism and log *P* Values of New Antihypertensive Thiomorpholinylmethylphenols: A Combined Experimental and Theoretical Study†

Karla Sanpedro-Montoya,‡ Beatriz Martínez-Pérez,§ Annia Galano,‡ Enrique Ángeles,§ Víctor H. Abrego,§ María Teresa Ramírez-Silva,‡ and Alberto Rojas-Hernández*,‡

Universidad Autónoma Metropolitana-Iztapalapa, Departamento de Química, Área de Química Analítica, Ap. Postal 55-534, San Rafael Atlixco 186, Col. Vicentina, 09340 México, D.F. México, and Universidad Nacional Autónoma de México, FES-Cuautitlán, Campo 1, Departamento de Ciencias Químicas, Laboratorio de Química Medicinal, Av. 1ero de Mayo S/N, Col. Sta. María las Torres, 54740 Cuautitlán Izcalli, Edo. de México, México

Four new antihypertensive thiomorpholinylmethylphenol compounds were synthesized by its potential antihypertensive and antiarhythmic properties. The pK_a values were determined experimentally, with the aid of program SQUAD, by Capillary Zone Electrophoresis (CZE) ($T = 310.15$ K and $I = 0.05$ mol·dm^{-3}) and by UV spectrophotometry at pseudophysiological conditions ($T = 310.15$ K and $I = 0.15$ mol·dm^{-3}), obtaining good agreement between the values determined with both techniques. A theoretical study was followed to propose a deprotonation mechanism for each compound. The log *P* values were also determined between *n*-octanol and water and compared with the values of other similar compounds to relate it with its possible biological activity.

Introduction

The most common treatment for fighting hypertension is through antihypertensive drugs. Nowadays there are a large number of such substances available. Unfortunately, most of them have adverse secondary effects. Therefore, the development and detailed study of new potential antihypertensive substances are of current and vital interest.

In 2006 Velázquez et al.[1] revisited the previous research by Stout et al.[2,3] and synthesized a new series of thiomorpholinylmethylphenol compounds. Some of them are shown in Table 1. They are intended to show antiarrhythmic and antihypertensive activity and low toxicity since their physicochemical properties and structure are similar to those of changrolin and its derivatives. However, there are no reported data on the acid constants of these thiomorpholinylmethylphenol compounds. Thus, it is the main aim of the present work to estimate them for the substances shown in Table 1, under pseudophysiological conditions of temperature and ionic strength, as well as to determine the log *P* values of these compounds between *n*-octanol and water, to compare them with those of similar compounds with demonstrated antihypertensive properties. It is also our purpose to propose a probable deprotonation mechanism for each of the studied compounds, i.e., to establish the relative order in which the deprotonation processes take place, following the same methodology described elsewhere.[4] It provides information on the prevailing structure at each pH interval, which is very important since different structures interact in different ways with the surrounding species present in biological environments. To establish the more plausible deprotonation mechanisms for the LQMs studied, the deprotonation paths shown in Scheme 1 were taken into account in this work.

Experimental Section

Reagents. NaOH (0.99, Merck) and HCl (0.37, Merck) were used to prepare acidic and basic solutions for spectrophotometric experiments and to adjust the pH of buffers in CZE. Methanol (spectroscopic grade, Baker), NaH_2PO_4 and Na_2HPO_4 (0.99, Fluka), Na_3PO_4 (0.96, Aldrich), and H_3PO_4 (0.854, Baker) were employed to prepare the buffers for CZE experiments or stock solutions of the LQMs synthesized. All aqueous solutions were prepared with deionized water (0.182 MΩ·m), purified with Millipore Milli-Q Gradient equipment.

General Synthesis Procedure. An appropriate substituted phenol (1 equiv), formaldehyde (2 equiv), and thiomorpholine (1 equiv) (solvent free) were mixed in a round flask fitted with a condenser. The mixture was irradiated with infrared light using a medicinal infrared lamp (250 W), and the reaction was monitored by thin-layer chromatography. The mixture was separated by column chromatography on silica gel using a hexane/ethyl acetate gradient solvent.[1]

4-Nitro-2-(thiomorpholin-1-ylmethyl)phenol (LQM324). Mp = (112 to 114) °C. Yield: 0.7. Reaction time: 25 min. ^{1}H NMR (200 MHz; $CDCl_3$; Me_4Si, δH): 9.44 (1H, s, OH), 8.10 (1H, m), 7.95 (1H, m), 6.86 (1H, m), 3.81 (2H, s), 2.83 (4H, m), 2.78, (4H, m). ^{13}C NMR (δC): 164.16, 140.19, 125.40, 124.85, 120.70, 116.52, 61.54, 54.30, 27.69. FAB-MS (M+1) 255 (1.00), 254 (0.60), 154 (0.30), 136 (0.25). Calculated for $C_{11}H_{14}N_2O_3S$: C(0.5195), H(0.0550), N(0.1102), O(0.1887), S(0.1261).

4-Hydroxy-3-(thiomorpholin-1-ylmethyl)benzonitrile (LQM330). Mp = (168 to 170) °C. Yield: 0.85. Reaction time: 15 min. ^{1}H NMR (200 MHz; $CDCl_3$; Me_4Si, δH): 8.22 (1H, s, OH), 7.47 (1H, m), 7.28 (1H, m), 6.84 (1H, m), 3.74 (2H, s), 2.85 (4H,

† Part of the "Sir John S. Rowlinson Festschrift".
* Corresponding author. E-mail: suemi918@xanum.uam.mx.
‡ Universidad Autónoma Metropolitana-Iztapalapa.
§ Universidad Nacional Autónoma de México.

10.1021/je100470g
Published on Web 08/03/2010

Table 1. Thiomorpholinylmethylphenol Ions of the Compounds Studied in This Work

Name of the synthesized compound	Formula of the synthesized compound	Fully protonated species
4-nitro-2-(thiomorpholin-1-ylmethyl)phenol	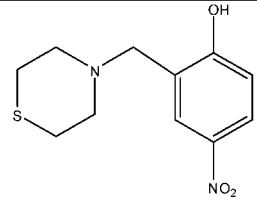 LQM324	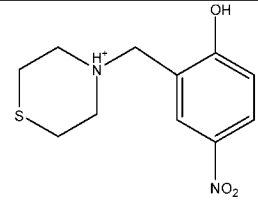 $H_2L^+ = H_2(lqm324)^+$
4-cyano-2-(thiomorpholin-1-ylmethyl)phenol	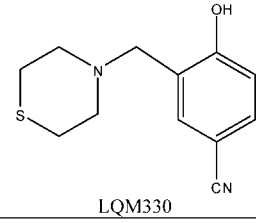 LQM330	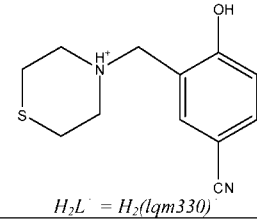 $H_2L^+ = H_2(lqm330)^+$
2-(thiomorpholin-1-ylmethyl)phenol	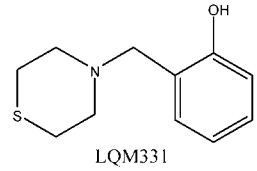 LQM331	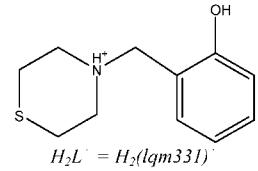 $H_2L^+ = H_2(lqm331)^+$
4-bromo-2-(thiomorpholin-1-ylmethyl)phenol	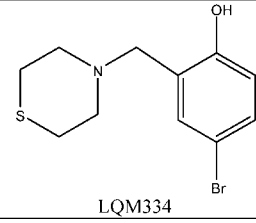 LQM334	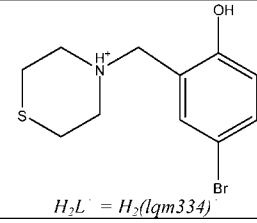 $H_2L^+ = H_2(lqm334)^+$

Scheme 1. (R = H, Br, CN, NO_2)

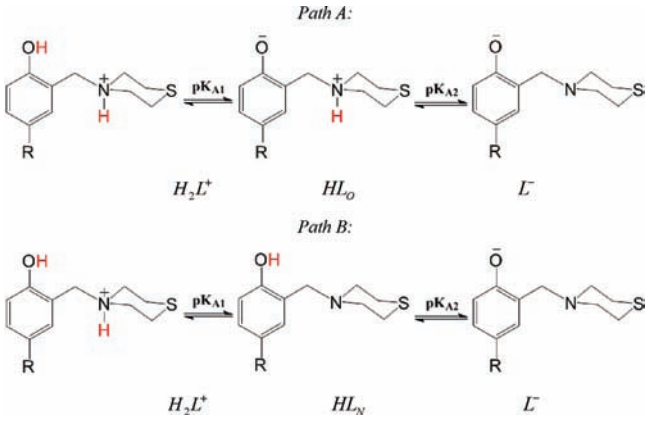

m), 2.76, (4H, m). ^{13}C NMR (δC): 162.04, 133.43, 132.70, 121.73, 119.31, 117.22, 102.38, 61.51, 54.33, 27.75. FAB-MS (M+1) 235 (0.70), 154 (1.00). Calculated for $C_{12}H_{14}N_2OS$: C(0.6151), H(0.0602), N(0.1196), O(0.0683), S(0.1368).

2-(Thiomorpholin-1-ylmethyl)phenol (LQM331). Mp = (120 to 121) °C. Yield: 0.82. Reaction time: 23 min. ^{1}H NMR (200 MHz; $CDCl_3$; Me_4Si, δH): 10.66 (1H, s, OH), 7.20 (1H, m), 6.95 (1H, m), 6.79 (1H, m), 3.71 (2H, s), 2.82 (4H, m), 2.71, (4H, m). ^{13}C NMR (δC): 157.58, 128.94, 128.76, 120.79, 119.27, 116.12, 62.27, 54.42, 27.93. FAB-MS (M+1) 210 (0.40), 106 (1.00). Calculated for $C_{11}H_{15}NOS$: C(0.6312), H(0.0722), N(0.0669), O(0.0764), S(0.1532).

4-Bromo-2-(thiomorpholin-1-ylmethyl)phenol (LQM334). Mp = (119 to 121) °C. Yield: 0.76. Reaction time: 18 min. ^{1}H NMR (200 MHz; $CDCl_3$; Me_4Si, δH): 10.66 (1H, s, OH), 7.20 (1H, m), 6.95 (1H, m), 6.79(1H, m), 3.71 (2H, s), 2.82 (4H, m), 2.71, (4H, m). ^{13}C NMR (δC): 157.58, 128.94, 128.76, 120.79, 119.27, 116.12, 62.27, 54.42, 27.93. FAB-MS (M+1) 288 (0.40), 184 (1.00). Calculated for $C_{11}H_{14}NOS$: C(0.4584), H(0.0490), Br(0.2772), N(0.0486), O(0.0555), S(0.1113).

In the precedent paragraphs, yield, relative strength of MS signals, and composition of compounds in their elements have been reported with the corresponding fractions, not percentages.

Capillary Zone Electrophoresis (CZE) Study. Conditions for the Electropherograms Acquisition. CZE experiments were achieved with a Beckman P/ACE MDQ with DAD equipment. A fused silica capillary with 50 μm of internal diameter, a total length (L_t) of 30.2 cm, and an effective length from injection to detector (L_d) of 20.0 cm on the long side or 10.2 cm on the short side was used. Sample injection was hydrodynamic using $6.89 \cdot 10^{-3}$ MPa (1 psi) by 10 s. Temperature was imposed at 310.15 K and voltage (V) at 20 kV (using reverse polarity only for pH < 3.1). Acetone was used as an electroosmotic flow marker and internal standard. pH of buffers was measured with a pH/Ion Analyzer (MettlerToledo) potentiometer and a combined pH electrode. Calibration of the potentiometer was achieved with three buffer standard solutions of 4.00, 7.00, and 10.00 (Radiometer Analytical).

Capillary Conditioning and Storing. At the beginning of the day, as usual, the capillary was washed with 0.1 mol·dm^{-3} NaOH during at least 5 min at 0.138 MPa, followed by another 5 min, at 0.138 MPa, wash with deionized water and a last 15 min, 20 psi, phosphate buffer wash (pH 7). Each run was started by a 1 min, 0.034 MPa, wash with 0.1 mol·dm^{-3} NaOH,

followed by a 1 min, 0.034 MPa, deionized water wash, then a 2 min, 0.034 MPa, phosphate buffer wash of the desired pH. The capillary was stored full of deionized water.

Buffers Employed and Stock Solutions of LQMs. Buffer pH solutions, 50 mmol·dm^{-3} in phosphates, were prepared by mixing adequate volumes of stock 0.50 mmol·dm^{-3} H_3PO_4, $H_2PO_4^-$, HPO_4^{2-}, or PO_4^{3-} aqueous solutions, adjusting finally the pH of each solution with 0.1 mol·dm^{-3} NaOH or HCl as required, before the filling of the 25.00 cm^3 volumetric flask to the mark. Individual solutions of LQM324, LQM330, LQM331, and LQM334 were prepared solving around 5 mg of each compound in the minimum amount of methanol before filling to the mark with deionized water the 50.00 cm^3 volumetric flask. Sample injected was added with acetone (as needed to have a 5 % acetone solution v/v).

Procedure to Obtain Effective Electrophoretic Mobility. At least three independent acquisitions of electropherogram were achieved for each pH value and compound. Effective electrophoretic mobilities (u_{eff}) were determined as the difference between the apparent (observed) mobility ($u_{app} = u_{LQM'}$)—related with the reciprocal of its migration time ($t_{LQM'}$)—and the mobility of the electroosmotic flow marker (u_{eof})—related with the reciprocal of its migration time (t_{eof})—in agreement with the equation[4,5]

$$u_{eff} = u_{app} - u_{eof} = u_{LQM'} = \frac{L_t L_d}{V}\left(\frac{1}{t_{LQM'}} - \frac{1}{t_{eof}}\right)$$

Spectrophotometric Study. Solution Preparation. An acidic solution, at an adequate concentration for spectrophotometric measurements, was prepared by solving a convenient mass of the LQM desired on a volume of 0.01 mol·dm^{-3} HCl with 0.14 mol·dm^{-3} NaCl aqueous mixture. Also, a basic solution was prepared by solving a convenient mass of the LQM desired on a volume of 0.01 mol·dm^{-3} NaOH with 0.14 mol·dm^{-3} NaCl aqueous mixture. Then, for each LQM, the acidic solution was titrated with the basic solution (and vice versa), to maintain the ionic strength (I) equal to 0.15 mol·dm^{-3} during titration. The temperature of the titration cell was maintained at 37 °C with a Cole−Parmer recirculator. Atmosphere over the solution was kept inert over passing a dry nitrogen flow.

pH Measurements. Solution pH, with a resolution of $\Delta pH = \pm 0.001$, was measured with a Tacussel LHP 430T potentiometer equipped with a Radiometer Analytical combined pH electrode F-69627. The pH of the solution was corrected by cell efficiency[6,7] with the equation[4]

$$pH_{corrected} = pH_{observed} + \left[\frac{pH_{calibration} - pH_{observed}}{pH_{calibration}}\right]Ef$$

Ef is an empirical parameter related to potentiometric cell efficiency that tends to zero while cell efficiency tends to 100 %. The results obtained with this equation are practically the same as those for the methods proposed by Wescott[6] or Bates.[7]

Conditions for the Absorption Spectra Acquisition. The absorption spectrum for each solution was achieved with a Perkin-Elmer Lambda 950 spectrophotometer, using quartz cells of 1 cm path length and a temperature of 310.15 K.

Equilibrium Constants Determination. The SQUAD program was used to obtain the formation constants by fitting UV absorption spectra[8,9] or effective electrophoretic mobilities[4,5] with pH and chemical composition of the solutions.

Determination of log P of LQM Compounds between n-Octanol and Water. Presaturation of Phases. *n*-Octanol (Baker) and deionized water obtained from a Milli-Q equipment of Millipore (0.182 MΩ·m) were presaturated to maintain the volume ratio constant during liquid−liquid extraction processes.

Calibration Curves. For each LQM compound, a calibration curve was prepared, by solving adequate amounts of each LQM in *n*-octanol presaturated with water.

An amount of 1 cm^3 of a LQM stock solution in *n*-octanol, with a concentration sited around the middle of the calibration curve, was mixed with 9 cm^3 of deionized water, presaturated with *n*-octanol. Vigorous stirring was undertaken during 5 min, and the phases were allowed to separate. A similar mixture in each case was used as a blank for absorbance measurements, but changing *n*-octanol presaturated of deionized water in place of the corresponding LQM stock solution. The UV absorption spectra for the *n*-octanol phase were recorded in the Perkin-Elmer Lambda 20 or 950 spectrophotometers, using quartz cells with an optical path length of 1 cm. The concentration of the corresponding LQM compound in the *n*-octanol phase was obtained by interpolation of the absorbance measured on the calibration curve, and this determination was repeated three times.

The linear regression equations of the calibration curves obtained were

$$A^{(315)} = (55.49 \pm 1.34)\cdot 10^{-3}([LQM324]o/mg\cdot dm^{-3}) + (-0.018 \pm 0.024) \text{ with } r^2 = 0.9989 \text{ for LQM324}$$

$$A^{(254)} = (76.85 \pm 4.25)\cdot 10^{-3}([LQM330]o/mg\cdot dm^{-3}) + (-0.015 \pm 0.045) \text{ with } r^2 = 0.9963 \text{ for LQM330}$$

$$A^{(275)} = (12.95 \pm 0.10)\cdot 10^{-3}([LQM331]o/mg\cdot dm^{-3}) + (0.0068 \pm 0.0061) \text{ with } r^2 = 0.9999 \text{ for LQM331}$$

and

$$A^{(287)} = (0.72 \pm 0.05)\cdot 10^{-3}([LQM334]o/mg\cdot dm^{-3}) + (0.007 \pm 0.011) \text{ with } r^2 = 0.9917 \text{ for LQM334}$$

where [LQM3XX]o represents the concentration of corresponding LQM in the octanol phase.

Extracted Fractions and log P Values. The extracted fractions of the corresponding LQM were obtained from the equation

$$E_{LQM3XX_o} = \frac{[LQM_{3XX}]_o}{[LQM_{3XX}]_{o,initial}}$$

and then its P values from the equation

$$\log P_{LQM3XX} = \log\left[\frac{1}{r}\left(\frac{E_{LQM3XX_o}}{1 - E_{LQM3XX_o}}\right)\right]$$

Computational Details. All the electronic calculations were performed with the Gaussian 03[10] package of programs. The stationary points were first modeled in the gas phase (vacuum), and solvent effects were included a posteriori by single-point calculations using the polarizable continuum model, specifically

Table 2. Deviation of the Calculated pK_a Values from the Experimental Data for the LQM331 System

ΔG_{gas}	ΔG_s	pK_{a1} (SE)[a]	pK_{a2} (SE)[a]	MUE[b]
CBS-QB3	PCM/HF/6-31+G(d,p)	10.28 (1.39)	11.57 (1.18)	1.29
CBS-QB3	PCM/HF/6-311++G(d,p)	10.19 (1.30)	11.51 (1.12)	1.21
CBS-QB3	CPCM/HF/6-31+G(d,p)	10.38 (1.49)	11.50 (1.11)	1.30
CBS-QB3	CPCM/HF/6-311++G(d,p)	10.28 (1.39)	11.44 (1.05)	1.22
CBS-QB3	CPCM/B3LYP/6-311++G(d,p)	9.84 (0.95)	14.91 (4.52)	2.74
B3LYP/6-311++G(d,p)	CPCM/HF/6-311++G(d,p)	10.49 (1.60)	10.54 (0.15)	0.88

[a] Signed error. [b] Mean unsigned error.

the integral-equation-formalism (IEF-PCM).[11−14] In PCM calculations, the choice of the solute cavity is important because the computed energies and properties strongly depend on the cavity size. In the present study, the cavity has been systematically built by the united atom model for the Hartree−Fock (UAHF) method[15] which is the recommended method for predicting free energies of solvation according to the Gaussian 03 User's Reference.[16]

Relative Gibbs free energies in solution have been computed using the Hess law and thermodynamic cycles, explicitly including solvation free energies (ΔG_s) From this cycle, the

$$\begin{array}{ccccc} HA_{(gas)} & \xrightarrow{\Delta G_{(x)}} & A^-_{(gas)} & + & H^+_{(gas)} \\ \uparrow {\scriptstyle -\Delta G_s(HA)} & & \downarrow {\scriptstyle \Delta G_s(A^-)} & & \downarrow {\scriptstyle \Delta G_s(H^+)} \\ HA_{(sol)} & \xrightarrow{\Delta G_{(s)}} & A^-_{(sol)} & + & H^+_{(sol)} \end{array}$$

Gibbs free energy of reaction in solution (ΔG_{sol}) can be obtained as the sum of the Gibbs free energy of reaction in vacuum (ΔG_{gas}) and the difference in solvation free energies ($\Delta\Delta G_s$)

$$\Delta G_{sol} = \Delta G_{gas} + \Delta\Delta G_s \quad (1)$$

where $\Delta\Delta G_s$ and ΔG_{gas} are calculated as

$$\Delta\Delta G_s = \Delta G_s(A^-) + \Delta G_s(H^+) - \Delta G_s(HA) \quad (2)$$

$$\Delta G_{gas} = G_{gas}(A^-) + G_{gas}(H^+) - \Delta G_{gas}(HA) \quad (3)$$

with ΔG_s representing the free energies of solvation. In all the cases, the reference state is 1M. For the cycles that involve protons, the $\Delta G_{gas}(H^+)$ and $\Delta G_s(H^+)$ values have been derived from experiments. We have used $\Delta G_{gas}(H^+) = -6.28$ kcal·mol^{-1} $= -26.28$ kJ·mol^{-1} and $\Delta G_s(H^+) = -264.61$ kcal/mol $= -1107.13$ kJ·mol^{-1}. This procedure has been previously used in calculation of pK_a values with successful results.[17−21]

The aqueous Gibbs free energies for the deprotonation reactions are in turn used to compute the acid equilibrium constant (K_a), according to

$$K_a = e^{-\Delta G_{sol}/RT} \quad (4)$$

Then, using the pK_a definition

$$pK_a = -\log(K_a) \quad (5)$$

This approach is based on the knowledge that computational methods poorly reproduce the solvation energies of protons, and it has been successfully used before by different authors.[21,22]

Different levels of theory have been tested, within this scheme, for LQM331 (R = H). The results are shown in Table 2. To choose a level of theory for computing ΔG_s, the ΔG_{gas} was calculated as accurately as possible (CBS-QB3). As this table shows, when the solvation energies are obtained using the B3LYP functional instead of HF a large error arises for the second pK_a. This is a logical finding since the UAHF method has been optimized for HF/6-31G(d).[15] Due to the size of the systems studied in the present work, an alternative, less computationally expensive method was tested for computing ΔG_{gas}: B3LYP/6-311++G(d,p). Even though the error in the first pK_a is larger than when calculating ΔG_{gas} with CBS-QB3, the error in the second one is smaller, leading to the lowest average error among all the tested methods.

On the basis of these results, the pK_a values for all the other systems were calculated using the last approach; i.e., geometry optimizations and frequency calculations were performed at the B3LYP/6-311++G(d,p) level of theory, followed by CPCM single-point calculations at the HF/6-311++G(d,p) level to obtain the ΔG_s values.

Results and Discussion

Stability of LQM Compounds. The stability studies on the four studied compounds were carried out by spectrophotometric analysis of their aqueous solutions that were followed in function of time for acid, basic, and neutral solutions. The cyano and nitro compounds (LQM330 and LQM324) showed higher stability than the other two (LQM331 and LQM334). The last compounds start to slowly precipitate after a few hours. On the basis of these results, we have used fresh solutions, prepared as diluted as possible.

Capillary Zone Electrophoresis (CZE) at T = 310.15 K and I = 0.05 mol·dm^{-3}. After the stability tests, the following step was the determination of the pK_a values of each LQM compound, at $T = 310.15$ K and $I = 0.05$ mol·dm^{-3} by capillary zone electrophoresis. The mobility curves as a function of pH are shown in Figure 1, and the parameters of their fitting with the program SQUAD, as explained elsewhere,[4,5] are shown in Table 3. An equation of the effective mobility as a function of pH for LQM species is presented in eq 5

$$u_{L'} = u_{L^-}f_{L^-} + u_{HL}f_{HL} + u_{H_2L^+}f_{H_2L^+} = \frac{u_{L^-} + u_{H_2L^+}[10^{(pK_{a1}+pK_{a2}-2pH)}]}{1 + 10^{(pK_{a2}-pH)} + 10^{(pK_{a1}+pK_{a2}-2pH)}} \quad (6)$$

where f_{L^-}, f_{HL}, and $f_{H_2L^+}$ are the molar fractions of the distribution diagram[23,24] of the LQM344 species; u_{L^-}, u_{HL} (that is equal to 0 because it is electrically neutral), and $u_{H_2L^+}$ are their corresponding ionic mobilities; and pK_{a1} and pK_{a2} are the minus logarithmic values of the acidity constants of H_2L^+ and HL species, respectively.

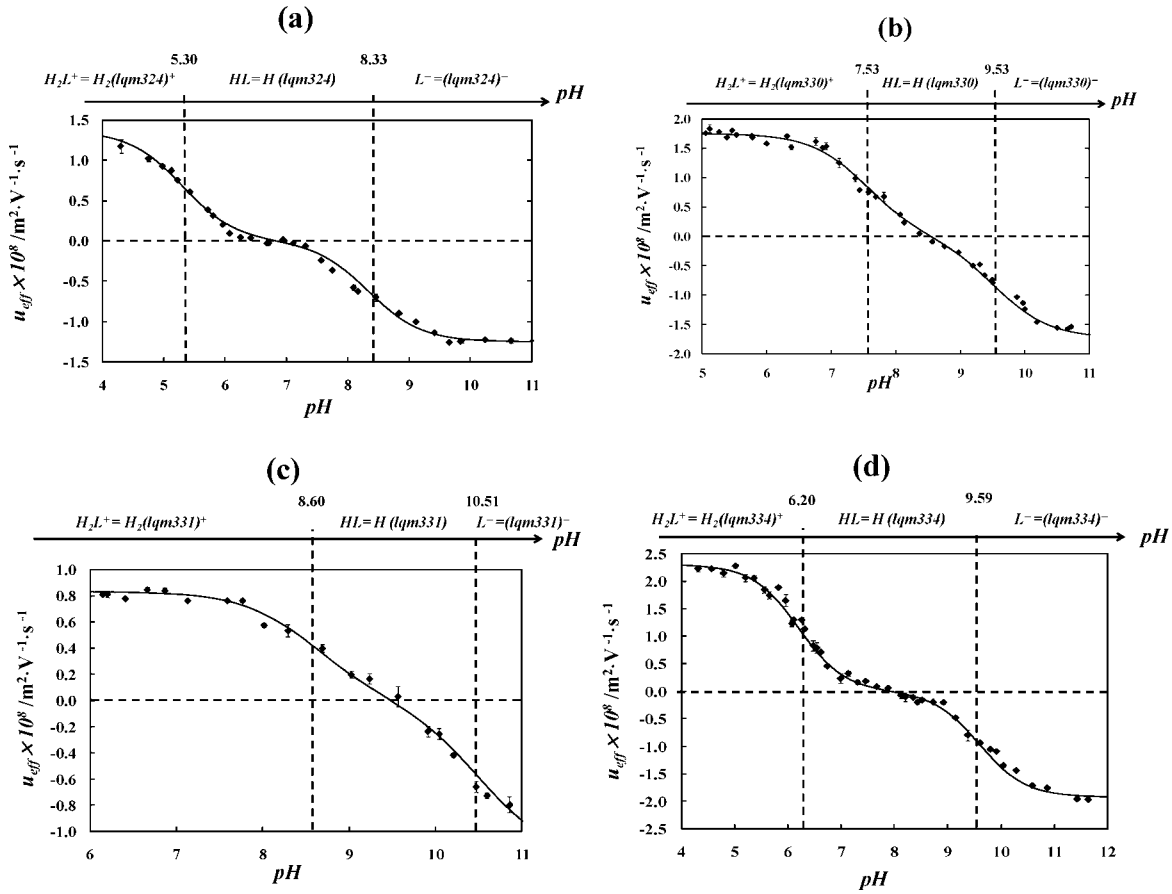

Figure 1. Effective mobility curves (u_{eff}) as function of pH, obtained at $T = 310.15$ K and $I = 0.05$ mol·dm^{-3}. The markers represent the experimental results, with error bars calculated as the standard deviation of three replicates, and the solid lines the fittings obtained with the aid of the program SQUAD. In the top of each figure, the corresponding predominance-zone diagram of species[23,24] is represented. (a) LQM324. (b) LQM330. (c) LQM331. (d) LQM334.

Table 3. pK_a Values for Acidity Equilibria and Effective Ionic Mobilities of Each Species $u_{H_j(lqm,3XX)z}$, Refined with SQUAD from Effective Electrophoretic Mobilities (u_{eff}, Figure 1) at $T = 310.15$ K and $I = 0.05$ mol·dm^{-3} [a]

compounds and related equilibria	pK_{ai}	[b] $u_{H_j(lqm3XX)z} \cdot 10^8$ / m^2·V^{-1}·s^{-1}	[c] $\lambda_{H_j(lqm3XX)z} \cdot 10^4$ / m^2·S·eq^{-1}
LQM324, $\sigma_{reg} = 0.032$[d]			
$H_2L^+ \rightleftarrows HL + H^+$	5.296 ± 0.018		
$HL \rightleftarrows L^- + H^+$	8.329 ± 0.129		
H_2L^+		1.367 ± 0.015	13.19 ± 0.14
L^-		-1.250 ± 0.115	12.06 ± 1.1
LQM330, $\sigma_{reg} = 0.019$[d]			
$H_2L^+ \rightleftarrows HL + H^+$	7.530 ± 0.002		
$HL \rightleftarrows L^- + H^+$	9.529 ± 0.019		
H_2L^+		1.750 ± 0.001	14.96 ± 0.01
L^-		-1.737 ± 0.006	16.76 ± 0.06
LQM331, $\sigma_{reg} = 0.008$[d]			
$H_2L^+ \rightleftarrows HL + H^+$	8.597 ± 0.006		
$HL \rightleftarrows L^- + H^+$	10.516 ± 0.003		
H_2L^+		0.831 ± 0.014	8.02 ± 0.13
L^-		-1.203 ± 0.002	11.60 ± 0.02
LQM334, $\sigma_{reg} = 0.013$[d]			
$H_2L^+ \rightleftarrows HL + H^+$	6.195 ± 0.009		
$HL \rightleftarrows L^- + H^+$	9.592 ± 0.001		
H_2L^+		2.305 ± 0.014	22.24 ± 0.13
L^-		-1.919 ± 0.115	18.5 ± 1.1

[a] Equivalent conductivities of each species $\lambda_{H_j(lqm3XX)z}$ have been calculated from $u_{H_j(lqm3XX)z}$. [b] The mobility of neutral species has been fixed to 0.000 m^2·V^{-1}·s^{-1} during refining. [c] λ values are calculated with equation $|z|\lambda_{H_j(lqm3XX)z} = Fu_{H_j(lqm3XX)z}$, where F accounts for the constant of Faraday.[4,5,25] [d] σ_{reg} represents the standard deviation of the regression.

All the compounds show the expected behavior (Figure 1). The double-protonated species correspond to a monocation ($H_2L^+ = H_2(lqm3XX)^+$), while the fully deprotonated one corresponds to a monoanion ($L^- = (lqm3XX)^-$). Nevertheless, it is noteworthy that on one hand the monoprotonated electrically neutral species (HL = H(lqm324) and H(lqm334)), for the nitro and bromo derivatives, respectively, reaches a maximum fraction ($f_{HL} \approx 0.95$) in its corresponding pH (6.8 and 7.9); on the other hand, this neutral species (HL = H(lqm330) and H(lqm331)) only reaches a maximum value around 0.82 in its corresponding pH (8.5 and 9.6) for the cyano and hydrogen derivatives. In other words, at physiological pH the neutral species predominates for the nitro and bromo derivatives, but the cation is the predominant species at these conditions for cyano and hydrogen derivatives.

UV Spectrophotometry at Pseudophysiological Conditions ($T = 310.15$ K and $I = 0.15$ M). Due to the potential medical applications of the studied compounds, the UV spectrophotometric study was carried out under pseudophysiological conditions: $T = 310.15$ K and $I = 0.15$ mol·dm^{-3}. The most representative spectra, in acidic and basic media, are shown in Figure 2. Several isosbestic points, corresponding to acid−base equilibra, are observed. This information, together with the data gathered from CZE for number and nature of species in aqueous solutions, allowed us to refine the same models with the program SQUAD.[8,9] The refined pK_a results are reported in Table 4, while the refined molar absorptivity coefficients are shown in Figure 3.

It is interesting to remark the similarity of the set of molar absorptivity coefficients of LQM331 and LQM334 species, while for LQM324 and LQM330 there are more differences. These could be attributed to the electro-attracting capacity of the substituent in the *para* position to the phenol group, greater

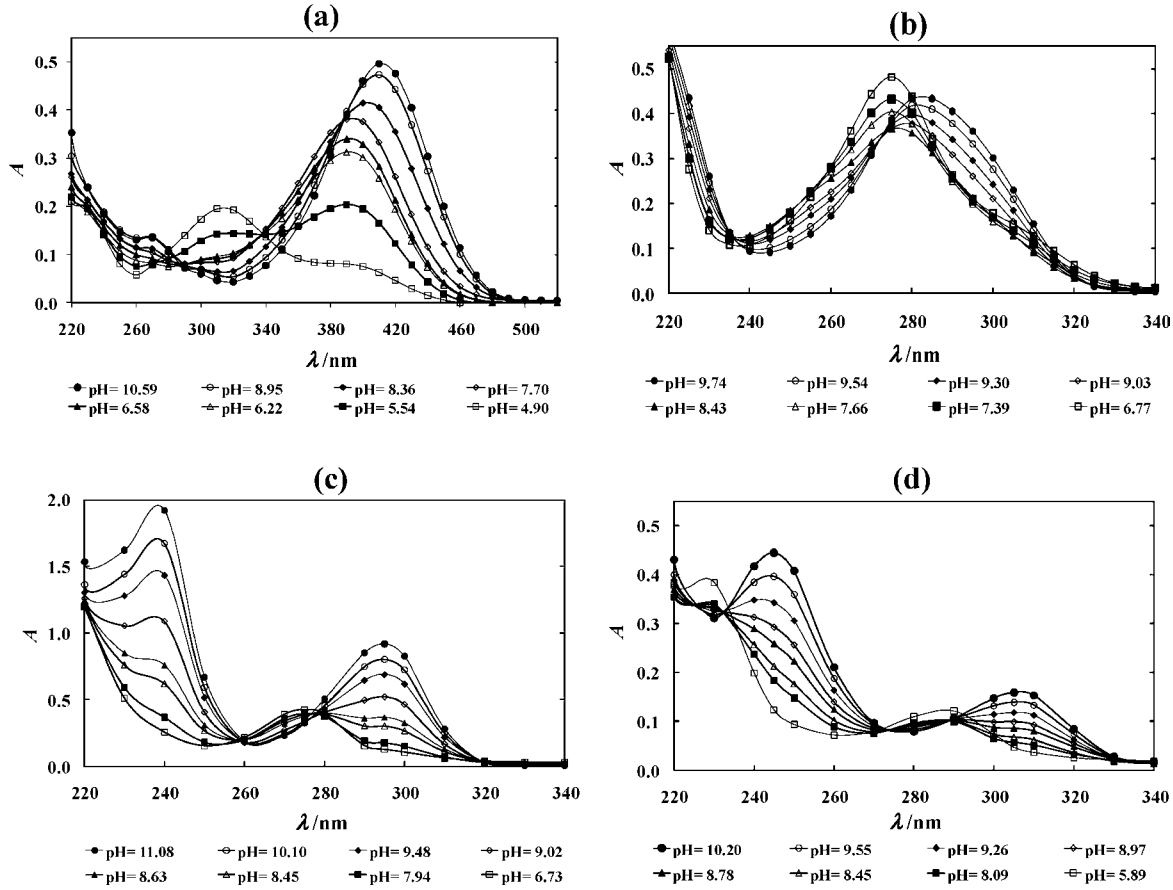

Figure 2. UV absorption spectra of (absorbance, A, as a function of wavelength, λ) LQM compounds studied in this work. (a) [LQM324] = $2.44 \cdot 10^{-5}$ mol·dm^{-3}. (b) [LQM330] = $4.61 \cdot 10^{-5}$ mol·dm^{-3}. (c) [LQM331] = $4.78 \cdot 10^{-5}$ mol·dm^{-3}. (d) [LQM334] = $3.85 \cdot 10^{-5}$ mol·dm^{-3}.

Table 4. pK_a Values Obtained under Pseudophysiological Conditions (T = 310.15 K and I = 0.15 mol·dm^{-3}), Refined with SQUAD from Spectrophotometric Data (Figure 2)

	p$K_{a1} \pm \sigma$	p$K_{a2} \pm \sigma$	σ_{reg}, U^a
LQM324	5.450 ± 0.001	8.412 ± 0.001	0.006, 0.038
LQM330	7.437 ± 0.008	9.380 ± 0.004	0.002, 0.008
LQM331	8.89 ± 0.11	10.391 ± 0.075	0.007, 0.032
LQM334	6.421 ± 0.032	9.261 ± 0.009	0.009, 0.019

[a] σ_{reg} represents the standard deviation of the regression, while U takes into account the sum of squares of the residuals.

for $-NO_2$ than for $-CN$ than for $-Br$. There is a bathochromic shift for all the wavelengths of maximum absorption for LQM324, as expected. Nevertheless, the differences in magnitude of molar absorptivity coefficients are difficult to explain because they are also related with the energy differences of the molecular orbitals involved in the electronic transition, in each case (and in each case they could be different).

In addition, we believe that the experimental pK_a values obtained spectrophotometrically are more accurate than those determined by electrophoresis because the imposition of ionic strength is better by the experimental task achieved (with NaCl in the first case and phosphate buffers in the latter). In fact, the differences observed in the pK_a values (up to 0.33) between the two methods should be attributed mainly to the different ionic strength values imposed in both cases.

Log P Values Obtained at Ambiance Temperature. Table 5 shows the comparison of log P values of LQM compounds studied in the present work with those calculated with the programs: ACDLogP of Adavanced Chemistry Development Laboratories, from Canada; ALOGPS 2.1 of VCC Laboratories, from Germany; miLogP of Molinspiration and KowWin of Syracuse Research Corporation (SRC), from USA.[26−29] As it can be seen in Table 5, there is great dispersion of the calculated values. In fact, ACDLogP and ALOGPS 2.1 programs fail for more than 0.15 log P units in two of the four LQMs studied, while the SRC program fails by the same amount in three of the four cases. The miLogP program fails for more than 0.15 log P units in all the LQMs studied. In other words, the different predictive methods render significantly different results for the same compound.

On the other hand, it seems that a bromine substituent in the LQM compounds originates higher solubility and affinity to the *n*-octanol phase, as it occurs with antihypertensive compounds with chloride substituents (e.g., losartan and felodipine), giving higher log P values than for the other substituents.

Theoretical Study of the Deprotonation Mechanisms. The LUMO density surfaces obtained for the H_2L^+ species are shown in Figure 4. According to this criterion, the site with the highest acid character depends on the *para* substituent in the phenol moiety. For those species with nitro and cyano substituents, the phenolic OH shows larger contribution to the LUMO density than the amino sites; i.e., the phenolic H is expected to be the most acid one and therefore the one involved in the first pK_a. For all the H and Br *para* substituents, the amino groups contribute to the LUMO densities in a larger proportion than the phenolic OH; i.e., the most acid sites are expected to be those in the thiomorpholine group. However, this is only a qualitative criterion, and a more detailed study based on Gibbs free energies is needed to establish, with a higher degree of certainty, the deprotonation mechanism.

Gibbs free energies for all possible deprotonation processes have been computed at 298.15 K. Table 6 shows the ΔG_{sol}

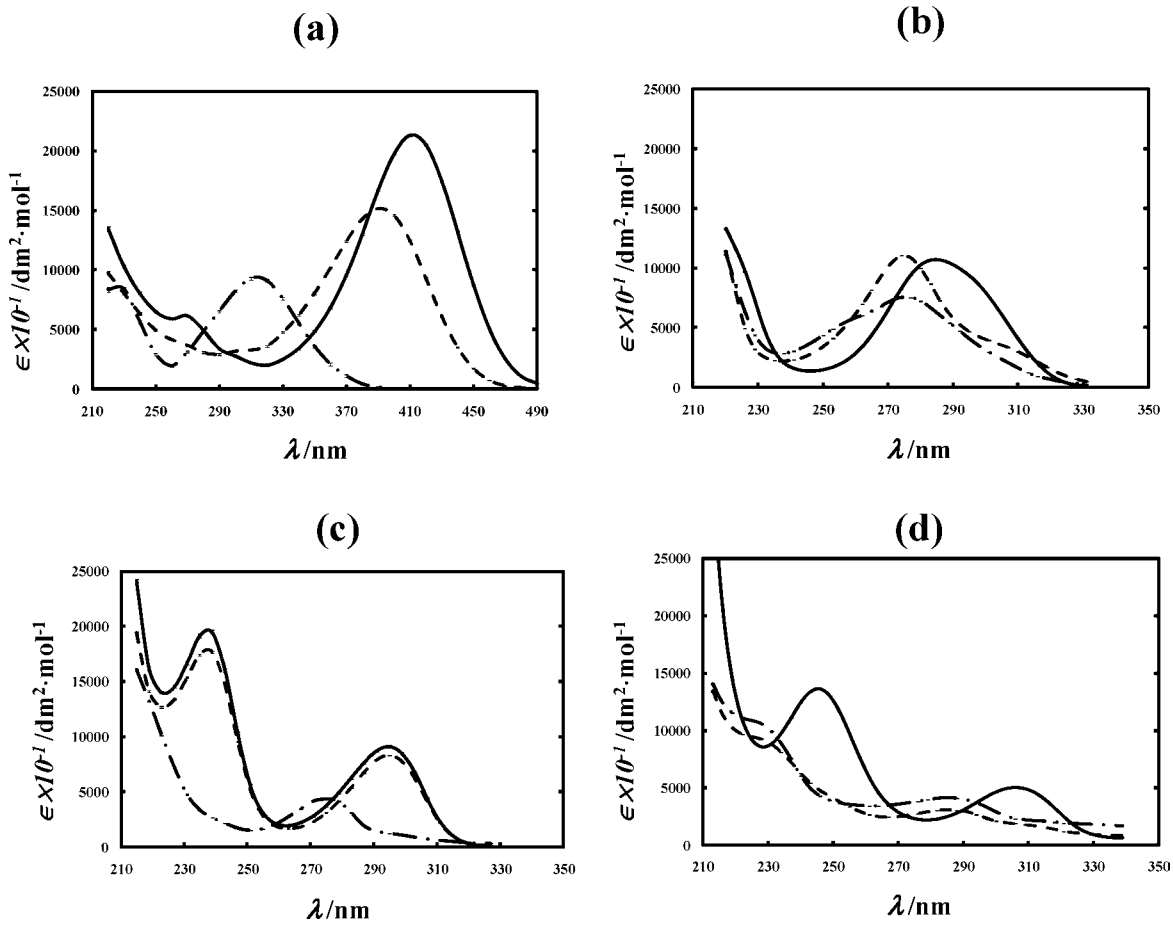

Figure 3. Absorptivity coefficients ε of the species of LQM compounds studied in this work, determined by the program SQUAD. (a) LQM324. (b) LQM330. (c) LQM331. (d) LQM334. Solid line (−) represents the absorptivity of L, dotted line represents the absorptivity of HL (- -) and segmented line (− - −) represents the absorptivity of H_2L^+.

Table 5. Experimental log *P* Values between *n*-Octanol and Water for LQM Compounds Studied in the Present Work and Calculated log *P* Values Calculated with Different Programs

	log *P*	log *P* calcd[a]			
substance	exptl	ACD LogP	ALOGPS 2.1	miLogP	KowWin SRC
LQM324	1.591 ± 0.016	1.53	1.77	2.00	2.13
LQM330	1.631 ± 0.009	1.56	1.67	1.80	1.83
LQM331	1.743 ± 0.038	1.45	1.78	1.07	1.73
LQM334	2.126 ± 0.017	2.45	2.58	2.85	2.62

[a] The uncertainties for the calculated values are 0.5 or greater.

values corresponding to the different pathways considered for the first deprotonation. These energy values are in good agreement with the predictions based on the LUMO density distribution. For the species with NO_2 and CN groups at the *para* sites of phenols, the most feasible process is the one involving the OH in the phenol group; i.e., the first pK_a should be associated with the acidity of this site. For all the other substituents, the pathways involving amino groups lead to more favorable processes, i.e., less endergonic.

Once the most viable path for the first deprotonation has been identified for H_2L^+ systems, the deprotonation routes are completely specified since only two deprotonation processes are considered. Accordingly, path A is proposed as the most viable one if R = CN or NO_2, and path B if R = H or Br.

The pK_a values calculated according to Scheme 2 are reported in Table 7. They are in good agreement with those obtained experimentally for pK_{a2} values and in some agreement for pK_{a1}

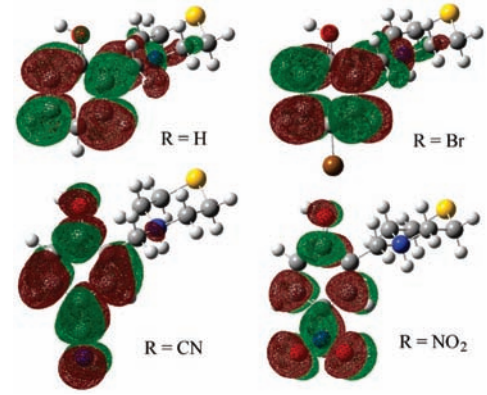

Figure 4. LUMO density surfaces, computed with isodensity value of 0.02 au.

Table 6. Gibbs Free Energies of Reaction in kJ·mol^{-1} for All Possible First Deprotonation Pathways at T = 298.15 K

	acid sites	
system	−OH	|−NH$^+$|
R = H	87.32	59.87
R = Br	84.52	41.30
R = CN	50.33	51.46
R = NO_2	39.71	51.38

values (Tables 3 and 4), probably due to the results obtained in the calibration procedure of the calculation method (see Section 2). A correlation between calculated and experimental pK_a values is shown in Figure 5 (without considering the pK_{a1} value

Scheme 2

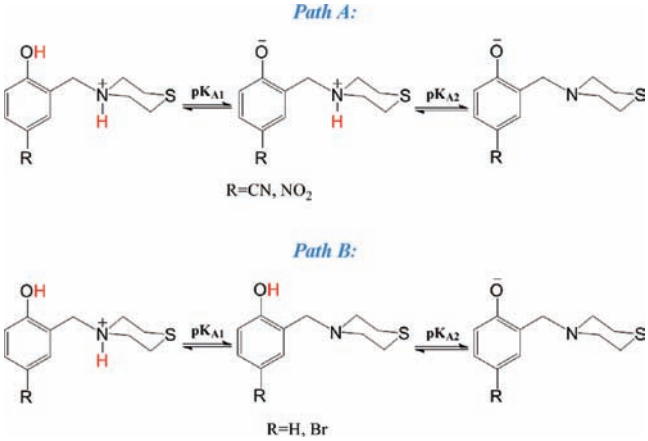

Table 7. Calculated pK_a Values, According to Pathways in Scheme 2

	pK_{a1}	pK_{a2}
R = H	10.49	10.54
R = Br	7.24	10.05
R = CN	8.82	9.40
R = NO_2	6.96	8.60

of LQM331). The theoretical calculations reproduce the experimental trends, although with a systematic error of about 1 unit for pK_{a1} value, which are also in line with chemical intuition. For instance, the presence of the nitro group at the *para* site of phenol significantly increases the acidity of the phenolic proton, which is explained by the high electrowithdrawing character of this substituent. Moreover, both pK_a values decrease when this substituent is present, which suggests that it also influences the acidity of the protons in the N atoms of thiomorpholine groups, despite the presence of a methylene group between thiomorpholine and the phenolic ring.

The deviations of the calculated pK_a values from those obtained by spectrophotometric and electrophoresis techniques are reported in Table 8 (without considering the pK_{a1} value of LQM331), in terms of mean signed errors (MSE), mean unsigned errors (MUE), and root-mean-square errors (RMSE). Since the theoretical chemical accuracy is generally accepted to be around 1 kcal·mol^{-1} = 4.184 kJ·mol^{-1}, for the highest levels of theory, and this would imply an error of about 0.73 units of pK_a, at T = 298.15 K, it can be stated that the present

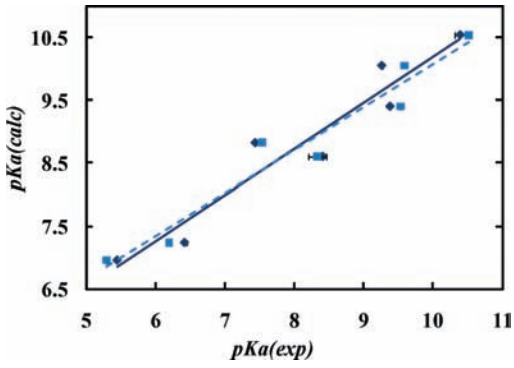

Figure 5. Correlation between calculated pK_a values, pK_a(calc), and experimental pK_a values, pK_a(exp), without considering the pK_{a1} value of LQM331. ◆, points that use pK_a values obtained by spectrophotometry; ■, points that use those obtained by CZE. Solid line (—) fits the equation pK_a(calc) = 0.732pK_a(exp) + 2.867 for spectrophotometric data, while the dotted line (---) fits the equation pK_a(calc) = 0.683pK_a(exp) + 3.241 for electrophoretic data.

Table 8. Mean Signed Errors MSE, Mean Unsigned Errors MUE, and Root-Mean-Square Errors RMSE, for Calculated pK_a Values with Respect to Those Estimated by Spectrophotometric and Electrophoresis Techniques, Without Considering the pK_{a1} Value of the LQM331 Compound

	spectrophotometry	electrophoresis
MSE	0.607	0.578
MUE	0.607	0.610
RMSE	0.676	0.721

calculations reproduce the experimental values. This agreement permits us to have some confidence in the used methodology, as well as in the theoretical predictions, and supports the elucidation of the deprotonation paths proposed above.

In summary, from the theoretical calculations, it can be proposed that the nature of the *para* substituent in the phenol group influences not only the acidity of the different protons (phenolic and thiomorpholinic) in H_2L^+ but also the route of the consecutive deprotonation processes.

Finally, the nature of the *zwitterionic* character of the neutral species could also be related to the differences in magnitude of molar absorptivity coefficients. The set of molar absorptivities of LQM331 is very similar to LQM344, and the neutral species seems to be non-zwitterionic in both cases. The differences are greater with the set of molar absorptivities of the species of LQM330 and LQM324, where the neutral species seems to be zwitterionic.

Conclusions

Stability tests of the studied compounds were found to safely choose the work concentrations and the titration conditions.

The pK_a values for the four antihypertensive studied compounds were determined by UV spectrophotometry at T = 310.15 K and I = 0.15 mol·dm^{-3} and CZE at T = 310.15 K and I = 0.05 mol·dm^{-3}.

These experimental results permit us to predict a better physiological behavior of LQM324 (nitro) and LQM334 (bromo) by the main predominance of its electrically neutral species in these conditions, even though the four LQMs studied in the present work follow at least the majority of the Lipinsky rules, for the development of drugs.[30]

The deprotonation mechanisms were elucidated using theoretical calculations. From the theoretical results, it can also be proposed that the nature of the *para* substituent in the phenol group influences not only the acidity of the different protons (phenolic and thiomorpholinic) but also the route of the consecutive deprotonation processes. The theoretical results permit us to propose that the neutral species of the Br derivative might confer lower solubility of these species with respect to the other derivatives, at physiological conditions, and this behavior was observed with the log P value determined experimentally.

Acknowledgment

A.G., M.T.R.-S., and A.R.-H. thank Laboratorio de Visualización y Cómputo Paralelo at UAM-Iztapalapa for the access to its computer facilities. E.A. also wants to acknowledge DGSCA for access to the KAMBALM supercomputer and to thank C. Barajas, F. Sotres, M. Hernández, R. Valadez, and D. Jiménez for their skillful technical assistance.

Literature Cited

(1) Velázquez, A. M.; Torres, L. A.; Díaz, G.; Ramírez, A.; Hernández, R.; Santillán, H.; Martínez, L.; Martínez, L.; Díaz-Barriga, S.; Abrego, V.; Balboa, M. A.; Camacho, B.; López-Castañares, R.; Dueñas-

González, A.; Cabrera, G.; Angeles, E. A novel one pot, solvent-free Mannich synthesis of methylpiperidinyl phenols, methylphenylmorpholinyl phenols and methylthiophenylmorpholinyl phenols using infrared light irradiation. *ARKIVOC* **2006**, *ii*, 150–161.

(2) Stout, D. M.; Mtier, W. L.; Barcelon-Yang, C.; Reynolds, R. D.; Brown, B. S. Synthesis and Antiarrhythmic and Parasympatholytic Properties of Substituted Phenols. 1. Heteroarylamine Derivatives. *J. Med. Chem.* **1983**, *26*, 808–813.

(3) Stout, D. M.; Mtier, W. L.; Barcelon-Yang, C.; Reynolds, R. D.; Brown, B. S. Synthesis and Antiarrhythmic and Parasympatholytic Properties of Substituted Phenols. 3. Modifications to the Linkage Region (Region 3). *J. Med. Chem.* **1985**, *28*, 295–298.

(4) Islas-Martínez, J. M.; Rodríguez-Barrientos, D.; Galano, A.; Ángeles, E.; Torres, L. A.; Olvera, F.; Ramírez-Silva, M. T.; Rojas-Hernández, A. Deprotonation Mechanism of New Antihypertensive Piperidinylmethylphenols: A Combined and Theoretical Study. *J. Phys. Chem. B* **2009**, *113*, 11765–11774.

(5) Rodríguez-Barrientos, D.; Rojas-Hernández, A.; Gutiérrez, A.; Moya-Hernández, R.; Gómez-Balderas, R.; Ramírez-Silva, M. T. Determination of pK_a values of tenoxicam from 1H-NMR chemical shifts and of oxicams from electrophoretic mobilities (CZE) with the aid of programs SQUAD and HYPNMR. *Talanta* **2009**, *80*, 754–762.

(6) Wescott, C. C. *pH Measurements*; Academic Press: Orlando, 1978.

(7) Bates, R. G. *Determination of pH*, 2nd ed.: Wiley: New York, 1973.

(8) Legget, D. J. *Computational Methods for Determination of Formation Constants*; Plenum Press: New York, 1985.

(9) Legget, D. J.; McBryde, W. A. E. General computer program for the computation of stability constants from absorbance data. *Anal. Chem.* **1975**, *47*, 1065–1070.

(10) Frisch, M. J.; Trucks, G. W.; Schlegel, H. B.; Scuseria, G. E.; Robb, M. A.; Cheeseman, J. R.; Montgomery, J. A., Jr.; Vreven, T.; Kudin, K. N.; Burant, J. C.; Millam, J. M.; Iyengar, S. S.; Tomasi, J.; Barone, V.; Mennucci, B.; Cossi, M.; Scalmani, G.; Rega, N.; Petersson, G. A.; Nakatsuji, H.; Hada, M.; Ehara, M.; Toyota, K.; Fukuda, R.; Hasegawa, J.; Ishida, M.; Nakajima, T.; Honda, Y.; Kitao, O.; Nakai, H.; Klene, M.; Li, X.; Knox, J. E.; Hratchian, H. P.; Cross, J. B.; Bakken, V.; Adamo, C.; Jaramillo, J.; Gomperts, R.; Stratmann, R. E.; Yazyev, O.; Austin, A. J.; Cammi, R.; Pomelli, C.; Ochterski, J. W.; Ayala, P. Y.; Morokuma, K.; Voth, G. A.; Salvador, P.; Dannenberg, J. J.; Zakrzewski, V. G.; Dapprich, S.; Daniels, A. D.; Strain, M. C.; Farkas, O.; Malick, D. K.; Rabuck, A. D.; Raghavachari, K.; Foresman, J. B.; Ortiz, J. V.; Cui, Q.; Baboul, A. G.; Clifford, S.; Cioslowski, J.; Stefanov, B. B.; Liu, G.; Liashenko, A.; Piskorz, P.; Komaromi, I.; Martin, R. L.; Fox, D. J.; Keith, T.; Al-Laham, M. A.; Peng, C. Y.; Nanayakkara, A.; Challacombe, M.; Gill, P. M. W.; Johnson, B.; Chen, W.; Wong, M. W.; Gonzalez, C.; Pople, J. A. *Gaussian 03*, revision E.01; Gaussian, Inc.: Wallingford, 2004.

(11) Cances, M. T.; Mennucci, B.; Tomasi, J. A new integral equation formalism for the polarizable continuum model: Theoretical background and applications to isotropic and anisotropic dielectrics. *J. Chem. Phys.* **1997**, *107*, 3032–3041.

(12) Mennucci, B.; Tomasi, J. Continuum solvation models: A new approach to the problem of solute's charge distribution and cavity boundaries. *J. Chem. Phys.* **1997**, *106*, 5151–5158.

(13) Mennucci, B.; Cances, E.; Tomasi, J. Evaluation of Solvent Effects in Isotropic and Anisotropic Dielectrics and in Ionic Solutions with a Unified Integral Equation Method: Theoretical Bases, Computational Implementation, and Numerical Applications. *J. Phys. Chem. B* **1997**, *101*, 10506–10517.

(14) Tomasi, J.; Mennucci, B.; Cances, E. The IEF version of the PCM solvation method: an overview of a new method addressed to study molecular solutes at the QM ab initio level. *J. Mol. Struct. (THEOCHEM)* **1999**, *464*, 211–226.

(15) Barone, V.; Cossi, M.; Tomasi, J. A new definition of cavities for the computation of solvation free energies by the polarizable continuum model. *J. Chem. Phys.* **1997**, *107*, 3210–3221.

(16) Frisch, Æ.; Frisch, M.; Trucks, G. W. *Gaussian 03 User's Reference*; Gaussian Inc.: Wallingford, 2003.

(17) Liptak, M. D.; Shields, G. C. Accurate pK_a Calculations for Carboxylic Acids Using Complete Basis Set and Gaussian-n Models Combined with CPCM Continuum Solvation Methods. *J. Am. Chem. Soc.* **2001**, *123*, 7314–7319.

(18) Liptak, M. D.; Gross, K. C.; Seybold, P. G.; Feldgus, S.; Shields, G. C. Absolute pK_a Determinations for Substituted Phenols. *J. Am. Chem. Soc.* **2002**, *124*, 6421–6427.

(19) Palascak, M. W.; Shields, G. C. Accurate Experimental Values for the Free Energies of Hydration of H^+, OH^-, and H_3O^+. *J. Phys. Chem. A* **2004**, *108*, 3692–3694.

(20) Murłowska, K.; Sadlej-Sosnowska, N. Absolute Calculations of Acidity of C-Substituted Tetrazoles in Solution. *J. Phys. Chem. A* **2005**, *109*, 5590–5595.

(21) Brown, T. N.; Mora-Diez, N. Computational Determination of Aqueous pK_a Values of Protonated Benzimidazoles (Part 1). *J. Phys. Chem. B* **2006**, *110*, 9270–9279.

(22) Llano, J.; Eriksson, L. A. First principles electrochemistry: Electrons and protons reacting as independent ions. *J. Chem. Phys.* **2002**, *117*, 10193–10206.

(23) Rojas-Hernández, A.; Ramírez, M. T.; González, I.; Ibanez, J. G. Predominance-Zone Diagrams in Solution Chemistry: Dismutation Processes in Two-Component Systems (M-L). *J. Chem. Educ.* **1995**, *72*, 1099–1105.

(24) Moya-Hernández, R.; Rueda-Jackson, J. C.; Ramírez, M. T.; Vázquez, G. A.; Havel, J.; Rojas-Hernández, A. Statistical Study of Distribution Diagrams for Two-Component Systems: Relationships of Means and Variances of the Discrete Variable Distributions with Average Ligand Number and Intrinsic Buffer Capacity. *J. Chem. Educ.* **2002**, *79*, 389–393.

(25) Bard, A. J.; Faulkner, R. *Electrochemical methods: fundamentals and applications*; Wiley: New York, 1980.

(26) ACDLogP is available from ACD Labs, Toronto, Canada, http://www.acdlabs.com/ (accessed July 8, 2010).

(27) VCCLAB, Virtual Computational Chemistry Laboratory, http://www.vcclab.org, 2005 (accessed July 8, 2010).

(28) miLogP is available from Molinspiration, at http://www.molinspiration.com (accessed July 8, 2010).

(29) KowWin is available from Syracuse Research Corporation (SRC), North Syracuse, USA at URL http://srcinc.com/what-we-do/product.aspx?id=138&terms=KowWin (accessed July 8, 2010).

(30) Lipinsy, C. A. Lead- and drug-like compounds: the rule-of-five revolution. *Drug Discovery Today* **2004**, *4*, 337–341.

Received for review May 4, 2010. Accepted July 19, 2010. We are indebted to UNAM through PAPIIT-IN218408, IN203609, and CONACyT 46124 and 82473 projects for partial financial support. K.S.-M. and A.R.-H. want to acknowledge CONACyT for a scholarship to follow postgraduate studies and support for sabbatical leave on FESC-UNAM during 2009, respectively.

JE100470G